Physics Letters B 814 (2021) 136088

Contents lists available at ScienceDirect

Physics Letters B

www.elsevier.com/locate/physletb

Beta decay of the axially asymmetric ground state of ^{192}Re

H. Watanabe [a,b,c,*], Y.X. Watanabe [c], Y. Hirayama [c], A.N. Andreyev [d,e], T. Hashimoto [f], F.G. Kondev [g], G.J. Lane [h], Yu.A. Litvinov [i], J.J. Liu [j], H. Miyatake [c], J.Y. Moon [f], A.I. Morales [k], M. Mukai [b,c,l], S. Nishimura [b], T. Niwase [b,m], M. Rosenbusch [c], P. Schury [c], Y. Shi [n], M. Wada [c], P.M. Walker [o]

[a] School of Physics, and International Research Center for Nuclei and Particles in Cosmos, Beihang University, Beijing 100191, China
[b] RIKEN Nishina Center, 2-1 Hirosawa, Wako, Saitama 351-0198, Japan
[c] Wako Nuclear Science Center (WNSC), Institute of Particle and Nuclear Studies (IPNS), High Energy Accelerator Research Organization (KEK), Wako, Saitama 351-0198, Japan
[d] Department of Physics, University of York, York, YO10 5DD, United Kingdom
[e] Advanced Science Research Center, Japan Atomic Energy Agency, Tokai-Mura, Naka-gun, Ibaraki 319-1195, Japan
[f] Rare Isotope Science Project, Institute for Basic Science (IBS), Daejeon 305-811, Republic of Korea
[g] Physics Division, Argonne National Laboratory, Lemont, IL 60439, USA
[h] Department of Nuclear Physics, Research School of Physical Sciences and Engineering, Australian National University, Canberra, ACT 0200, Australia
[i] GSI Helmholtzzentrum für Schwerionenforschung GmbH, 64291 Darmstadt, Germany
[j] Department of Physics, the University of Hong Kong, Pokfulam Road, Hong Kong
[k] Instituto de Física Corpuscular (CSIC-Universitat de Valencia), Apartado Correos 22085, E-46071 Valencia, Spain
[l] University of Tsukuba, Tsukuba, Ibaraki 305-0006, Japan
[m] Department of Physics, Kyushu University, Fukuoka 819-0395, Japan
[n] Department of Physics, Harbin Institute of Technology, Harbin 150001, China
[o] Department of Physics, University of Surrey, Guildford GU2 7XH, United Kingdom

ARTICLE INFO

Article history:
Received 20 October 2020
Accepted 18 January 2021
Available online 21 January 2021
Editor: D.F. Geesaman

Keywords:
^{192}Re
β decay
Axial asymmetry
Shape transition

ABSTRACT

The β decay of $^{192}_{75}\mathrm{Re}_{117}$, which lies near the boundary between the regions of predicted prolate and oblate deformations, has been investigated using the KEK Isotope Separation System (KISS) in RIKEN Nishina Center. This is the first case in which a low-energy beam of rhenium isotope has been successfully extracted from an argon gas-stopping cell using a laser-ionization technique, following production via multi-nucleon transfer between heavy ions. The ground state of ^{192}Re has been assigned $J^{\pi} = (0^{-})$ based on the observed β feedings and deduced $\log ft$ values towards the 0^{+} and 2^{+} states in ^{192}Os, which is known as a typical γ-soft nucleus. The shape transition from axial symmetry to axial asymmetry in the Re isotopes is discussed from the viewpoint of single-particle structure using the nuclear Skyrme-Hartree-Fock model.

© 2021 The Authors. Published by Elsevier B.V. This is an open access article under the CC BY license (http://creativecommons.org/licenses/by/4.0/). Funded by SCOAP[3].

One of the key aspects of atomic nuclei is that a variety of geometrical shapes manifest themselves depending on the configurations of the constituent protons and neutrons, which interact with each other through the strong nuclear force in a finite space. The deformation in the nuclear equilibrium shape is an exemplary case of the spontaneous symmetry breaking [1] that can be found in many areas of physics. In this context, the study of deformed nuclear matter and the associated collective motion has a broad scope.

Given axially symmetric deformations like prolate (elongated) and oblate (flattened) ellipsoidal shapes, the systems are invariant under a rotation around the symmetry axis. The rotational invariance is broken in nuclei having three different radii in the intrinsic coordinates. The degree of triaxial distortion, represented by the angular variable γ, tends to be developed in regions where shape transitions and/or coexistence between prolate and oblate deformations can take place [2–6]. Since, however, the occurrence of well-established asymmetric shapes is rather rare compared to the large abundance of axially symmetric (in particular, prolately deformed) cases, the exploration of some nuclei that are triaxial in their ground states is a long-standing challenge in nuclear structure physics.

* Corresponding author at: School of Physics, and International Research Center for Nuclei and Particles in Cosmos, Beihang University, Beijing 100191, China.
E-mail address: hiroshi@ribf.riken.jp (H. Watanabe).

https://doi.org/10.1016/j.physletb.2021.136088
0370-2693/© 2021 The Authors. Published by Elsevier B.V. This is an open access article under the CC BY license (http://creativecommons.org/licenses/by/4.0/). Funded by SCOAP[3].

Concerning axial asymmetry in medium-heavy and heavy nuclei, $^{192}_{76}Os_{116}$ and its vicinity have attracted considerable interest both experimentally and theoretically. The second 2^+ state at 489 keV in ^{192}Os is the lowest in energy of the 2^+_2 levels ever identified as the bandhead of the (quasi) γ band for even-even nuclei throughout the chart of nuclides, indicating that this nucleus is an especially promising candidate for enhanced ground-state axial asymmetry [7]. However, neither the rigid triaxial rotor nor the large-amplitude fluctuation in the γ direction, two extreme pictures of axially asymmetric nuclei, are adequate to reproduce $E2$ matrix elements extracted from Coulomb excitation of ^{192}Os [8]. The γ-soft properties of even-even nuclei in this shape transitional region can be explained well as being almost exactly intermediate between the two geometrical limits, using the interacting boson model Hamiltonian determined with energy density functionals [9,10]. Such γ softness causes the mixing of configurations with different K values, the angular momentum projection on the symmetry axis of an axial shape, and thereby results in a serious violation of K-forbidden transitions involved in radioactive decays, as observed for the $J^\pi = K^\pi = (10^-)$ isomer in ^{192}Os [7].

In this Letter, we report on the β decay from $^{192}_{75}Re_{117}$ to ^{192}Os. Although the same decay channel was studied before [11,12], the β-decay intensities and $\log ft$ values have never been evaluated. The present work focuses in particular on the previously unreported spin-parity assignment for the ground state of the parent nucleus ^{192}Re. From theoretical point of view, there are two local minima being almost equal in depth at prolate and oblate deformations on the potential energy curve calculated for ^{192}Re [13]. However, the shape of each state in such a "critical-point" nucleus depends sensitively on the deformed single-particle structure. Total Routhian Surface calculations for ^{192}Re predict the prolate ground state with a high-K configuration, which coexists with an oblate shape that is stabilized by the rotation alignment of the unpaired proton and neutron in the high-j orbitals [14].

Experimentally, it is still difficult to produce ^{192}Re even at modern radioactive-isotope-beam (RIB) facilities [15,16]. A currently utilized method to synthesize heavy neutron-rich nuclei in this mass region is cold fragmentation of ^{208}Pb beams at 1 GeV per nucleon at GSI [17]. Following this, isomeric states were discovered in ^{192}Re [18,19]. Another choice to get access to this hard-to-reach area approaching the $N = 126$ shell closure is to employ heavy-ion-induced multi-nucleon transfer (MNT) reactions with neutron-rich (stable) isotopes [20,21]. In conjunction with a gas-cell arrangement in which the reaction products are stopped/ionized and with subsequent mass separation, one can obtain low-energy RIBs even for refractory elements that are hard to be vaporized. This article presents the first successful extraction of Re ions using a new RIB-production scheme based on the MNT method, the KEK Isotope Separation System (KISS) [22–24].

A RIB of ^{192}Re was produced via MNT between a 50-pnA projectile of ^{136}Xe and a natural Pt target with a thickness of 10.7 mg/cm^2. The 10.75-MeV/u primary beam from the RIKEN Ring Cyclotron was decelerated to 8.8 MeV/u after passing through Ti degraders placed in front of the Pt target to optimize the production of the target-like fragments. The reaction products were thermalized and neutralized in a doughnut-shaped gas cell filled with high-pressure (80 kPa) gaseous argon, and then transported by a gas flow to the cell outlet, where a two-color, two-step resonant laser ionization technique is applied for an unambiguous selection of a single element. The singly charged ^{192}Re$^+$ ions were extracted through the RF ion guides and reaccelerated to 20 keV, followed by mass separation using the KISS spectrometer. The reader is referred to [25,26] for more technical details and the recent status of KISS.

During 4.2 days of data run, about 1.5×10^5 ^{192}Re nuclides were collected with an average intensity of 0.3 particle/s on a

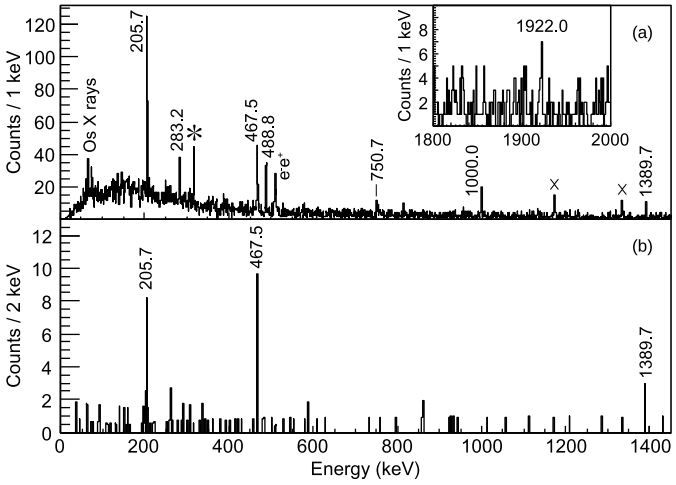

Fig. 1. (a) γ-ray energy spectrum measured in coincidence with MSPGC following implantation of ^{192}Re. Transitions in ^{192}Os are labeled with their energy values, while γ-ray peaks that originate from the room background and beam contaminants are marked with crosses and asterisk, respectively. The inset magnifies a high-energy region. (b) Energy projection of β-delayed γ-ray coincidence events measured with a sum of gates on the 283- and 489-keV γ rays in ^{192}Os.

12-μm-thick aluminized mylar tape of a tape-transport system installed at the end of the KISS beamline. The decay measurements were carried out with three different beam-on/off conditions of 90/180, 24/48, and 45/15 s in order to accommodate decays both from the ground state ($T_{1/2} = 16(1)$ s [11]) and from a previously reported long-lived isomer ($T_{1/2} = 61^{+40}_{-20}$ s [19]) in ^{192}Re. The implantation position was surrounded by a multi-segmented proportional gas counter (MSPGC) that covered 80% of the 4π solid angle with two layers of 16 counters [27]. This layered arrangement of the counters served to distinguish between high-energy β rays and low-energy internal-conversion electrons. Each element of MSPGC has a capability of position correlation in the vertical direction using the pulse-height information taken from both ends of the counter. The MSPGC was surrounded by four large-volume Clover-type HPGe detectors in a close geometry, having a γ-ray add-backed full-energy peak efficiency of 7.8% at 1 MeV. The implementation of a highly efficient detection system enabled β-γ-γ coincidence analyses.

It is to be remarked that no events relevant to the decay from a long-lived isomer in ^{192}Re, which was identified at $E_x = 267(10)$ keV with $T_{1/2} = 61^{+40}_{-20}$ s for highly charged ions in the GSI Experimental Storage Ring (ESR) [19], have been observed in the present work, despite a careful inspection with the sufficient statistics. A possible reason for its non-observation is that the isomeric half-life in ^{192}Re is much shorter than the mean extraction time from the KISS system ($\sim$ 500 ms [24]). Such a change in lifetime can be caused by suppression of internal conversion in highly charged ions [28]. Thus, the decay scheme from this isomer remains unclear, and we report only on the results of β-decay spectroscopy of the ^{192}Re ground state below.

Fig. 1(a) shows an example of the β-delayed γ-ray coincidence spectrum measured in the present work. The efficiency-corrected γ-ray intensities relative to the most intense 206-keV transition are summarized in Table 1. Observed were the $2^+_{1,2}$ and 0^+_2 states, being consistent with the previous β-decay study [11]. The γ-branching ratios deduced for the 2^+_2 and 0^+_2 levels are also consistent with the reference values [11]. In addition, β feedings towards other known excited states at 1206, 1879, and 2128 keV have been identified by the observation of γ rays that were reported to de-excite these levels [11]. Based on these observations, the decay scheme of ^{192}Re was constructed as displayed in Fig. 2, where the spins and parities of the ^{192}Os levels are presented if they

Table 1
Summary of transitions in ^{192}Os populated via the β decay from ^{192}Re.

E_γ (keV)	I_γ (rel.)[a]	Initial state		Final state	
		E_x (keV)	J^π	E_x (keV)	J^π
205.7	100	205.7	2_1^+	0.0	0_1^+
283.2	28(6)	488.8	2_2^+	205.7	2_1^+
467.5	53(8)	956.4	0_2^+	488.8	2_2^+
488.8	61(9)	488.8	2_2^+	0.0	0_1^+
750.7	17(7)	956.4	0_2^+	205.7	2_1^+
1000.0	51(10)	1205.6	0_3^+	205.7	2_1^+
1389.7	27(7)	1878.5		488.8	2_2^+
1922.0	9(5)	2127.7		205.7	2_1^+

[a] Relative to the γ-ray intensity of the 206-keV transition.

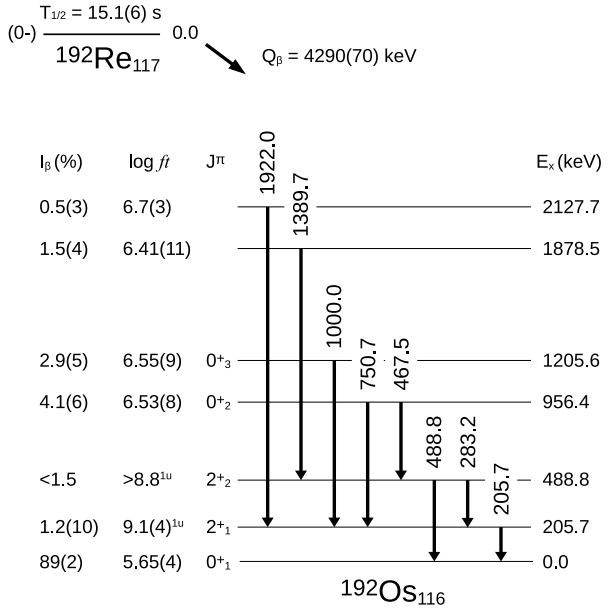

Fig. 2. Level scheme of ^{192}Os populated in the β decay of ^{192}Re. The values of excitation energy (E_x), spin and parity (J^π), β-decay intensity (I_β), and logft are given on the right- and left-hand sides of each level. For the levels of ^{192}Os, J^π are taken from [11] if they are firmly assigned. For the ground state of ^{192}Re, $T_{1/2} = 15.1(6)$ s and $J^\pi = (0^-)$ are obtained in the present work, while $Q_\beta = 4290(70)$ keV is taken from [29]. The superscript "1u" indicates first-forbidden unique β decay.

are firmly assigned in [11]. The 1879-keV state was previously assigned (2^+) with a branch towards the 4_3^+ state at 1070 keV [11]. However, the spin-parity assignment for this state is not given in Fig. 2 since neither the transition feeding nor deexciting the 4_3^+ state could be observed in the present β-decay measurement. Another γ-decay branch of 1390 keV from the 1879-keV level to the 2_2^+ state [11] has been confirmed by a γ-γ coincidence analysis, as demonstrated in Fig. 1(b).

The β-branching ratio I_β to each excited state was derived from an imbalance of the total intensities $(1+\alpha_T)I_\gamma$, where α_T denotes the total conversion coefficient [30], between the incoming and outgoing transitions. Similarly, the β-branching ratio to the ground state was determined to be 89(2)% from the difference between the total number of β particles associated with the ^{192}Re decay by a fit to the growth-decay curves and the sum of the 206- and 489-keV total transition intensities. In this analysis, possible contributions from (unobserved) $E0$ transitions between the 0^+ states were omitted. However, the argument on spin-parity assignment given below should be unaltered with the lack of allowance for $E0$ transitions since their relative intensities are most likely negligible, as observed for ^{188}Os and ^{196}Pt [31]. It should be noted that the values of I_β given in Fig. 2 are considered as upper limits,

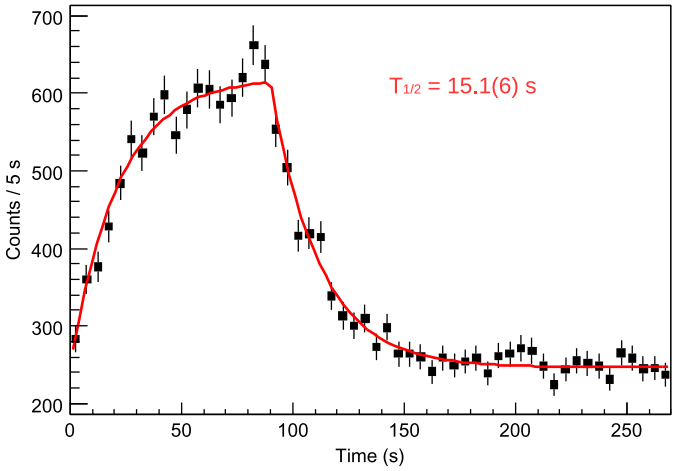

Fig. 3. Time distributions of β rays measured with MSPGC. The measurement of the growth and decay curves was carried out using macroscopically pulsed ^{192}Re$^+$ beams at 20 keV with an on/off condition of 90/180 s. The red solid line represents the result of a log-likelihood fit.

due to possible unobserved feedings from higher-lying states. The corresponding (lower limits of) logft values were calculated using $Q_\beta = 4290(70)$ keV [29] and a half-life of 15.1(6) s measured in the present work with better precision than in the previous work [11], as shown in Fig. 3.

The evaluated logft values put constraints on the spin-parity assignment for the parent β-decaying state. A strong β-decay branch towards the 0^+ ground state of ^{192}Os should favor an assignment of 0^+ or 0^- for the ground state of ^{192}Re. ($J^\pi = 1^\pm$ assignment is unlikely due to $I_\beta \approx 0$ for feeding the $2_{1,2}^+$ states.) However, the possibility of 0^+ can be ruled out since the β-decay branches to the 0_1^+ states in ^{192}Os have much smaller logft values than all known "isospin forbidden" $0^+ \to 0^+$ β transitions in heavy nuclei (see Table 4 in [32]). The value of logft obtained for feeding the ^{192}Os ground state is comparable to logft = 5.75 and 5.18 measured before for the $0^- \to 0^+$ first-forbidden non-unique transitions involved in the β decays of ^{196}Ir [33] and ^{206}Tl [32], respectively. Based on these observations, the ground state of ^{192}Re is assigned tentatively $J^\pi = (0^-)$.

In the neutron-rich $A \approx 190$ region, the ground-state properties of even-even nuclei have been theoretically investigated within the mean-field framework using a variety of interactions and forces [6,35,36]. There are slight differences in the position and depth of deformed minima on the potential energy surfaces constrained by the quadrupole deformation variables β and γ, depending on the interactions/functionals used in the calculations. However, the overall trend of prolate-to-oblate shape transitions passing through γ-soft nuclei with increasing the number of neutrons is predicted in common for the even-even $_{74}$W, $_{76}$Os, and $_{78}$Pt nuclei.

The odd and odd-odd systems are also of significance in understanding the shape-polarization effects by the unpaired nucleons, yet they have been scarcely studied in the self-consistent mean-field approach in this mass region. To interpret the low-lying level structure in the $_{75}$Re isotopes approaching $N = 116$, which is supposed to be the critical neutron number for the occurrence of ground-state prolate-to-oblate shape transition and enhanced γ softness, we have performed Skyrme-Hartree-Fock (SHF) calculations using the symmetry-unrestricted HFODD code [37].

At first, the low-energy excitation spectra are calculated for odd-A Re isotopes and compared to the experimental observables, as a benchmark for testing various Skyrme functionals available in HFODD ver. 2.73y [38]. The observed excitation energies of low-lying $J^\pi = 1/2^+$, $9/2^-$, and $5/2^+$ states are plotted as a function

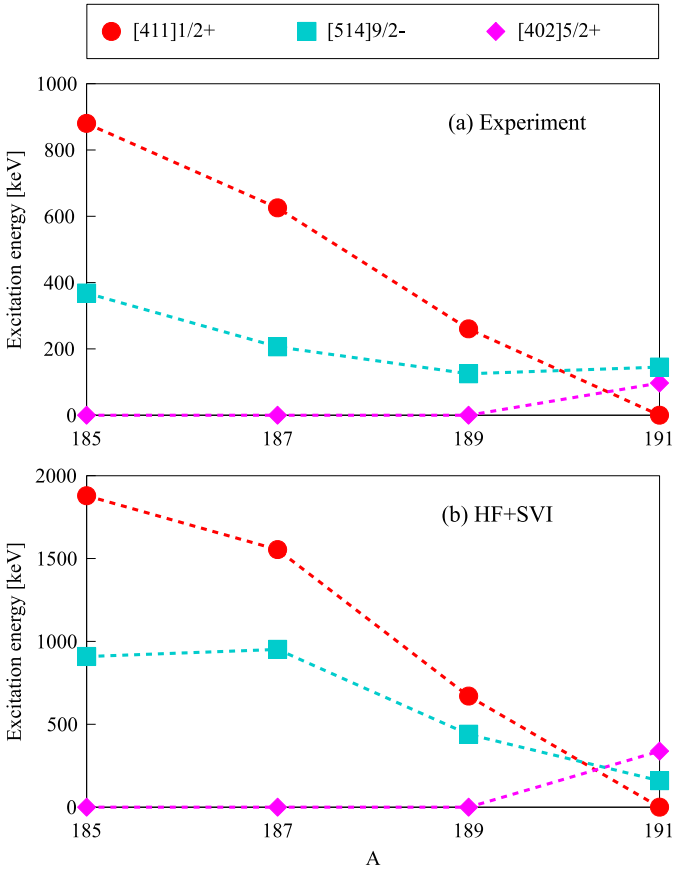

Fig. 4. Energy systematics of low-lying levels for odd-A Re isotopes. (a) Observed excitation energies of the proton one-quasiparticle states associated with Nilsson orbitals as indicated above. The experimental data are taken from [34]. (b) Similar to (a), but plotted are the relative energies of the HF states calculated with the SVI functional. The filled circles, squares, and diamonds correspond to the given configurations, in which the asymptotic quantum numbers, $[411]1/2^+$, $[514]9/2^-$, and $[402]5/2^+$, are the dominant components of the respective wave functions. The dashed lines connecting the same symbols are a guide to the eye.

of the mass number from 185 to 191 in Fig. 4(a). These levels are interpreted as being of proton one-quasiparticle nature associated with the Nilsson orbitals, $[411]1/2^+$, $[514]9/2^-$, and $[402]5/2^+$, respectively [34]. A remarkable feature in this plot is that the $1/2^+$ level falls rapidly in energy relative to the $5/2^+$ and $9/2^-$ states with increasing mass number and it becomes the ground state in ^{191}Re. The observed systematic trends can be reproduced fairly well by the SHF calculations with the use of the SVI functional [39], as demonstrated in Fig. 4(b). We have confirmed that the general tendency of the odd Re isotopes considered here can be reproduced to a certain extent by the calculations with other Skyrme interactions, such as SkM* [40], SLy4 [41], and SkP [42], but the calculation with SVI is a much better description than the others. It should be noted that Fig. 4(b) displays the calculated relative energies of the HF states, each of which has the largest overlap with the asymptotic state $[411]1/2^+$, $[514]9/2^-$, or $[402]5/2^+$. Since the pairing correlations are not taken into account, the calculated energies are about twice as large as the corresponding experimental excitation energies. However, the fair agreement in qualitative behavior between the experimental and theoretical single-particle spectra validates to employ the HF+SVI calculations for discussing the properties of low-lying levels in this transitional region.

In the previous work [34], the rapid decrease in energy of the $[411]1/2^+$ level that forms the ground state in ^{191}Re was discussed based on the Nilsson model with the inclusion of a hexadecapole deformation. The present SHF calculations, in which the hexadecapole component is also taken into account, reveal that the γ deformation plays a pivotal role in the level evolution in terms of the single-particle orbitals near the Fermi surface. In Fig. 5, the single-particle energies (SPEs) are described as functions of the positive (prolate) and negative (oblate) axial quadrupole moments Q_{20}, which are connected through the γ deformation parameter for constant $Q_{20} = 12$ b. For protons, it can be seen that the two positive-parity orbitals labeled with the numbers 19 and 20 in squares, which are counted from the bottom of the potential well, approach each other with increasing γ and repel around $\gamma = 30°$, while the SPE of the 18th negative-parity orbital is almost constant for the entire range of γ. According to the current SHF prediction, as summarized in Table 2, the dominant Nilsson component of the "active" single-proton orbital in the ground-state configuration, *i.e.*, the 20th positive-parity orbital, changes from $[402]5/2^+$ to $[411]1/2^+$ between ^{189}Re and ^{191}Re, consistent with the observed systematics. This phenomenon mirrors an exchange of the single-particle properties between the 19th and 20th positive-parity levels through the orbital repulsion at $\gamma \approx 30°$. Note that the calculated spin values in Table 2 are not necessarily a half-integer unless the nucleus has an axially symmetric ($\gamma = 0°$ or 60°) shape on account of the K-mixing.

Table 2
Calculated spins, intrinsic quadrupole moments Q_2, and degrees of triaxial deformation γ for the lowest-lying states of odd-A $_{75}$Re isotopes. The 5th column shows the asymptotic quantum numbers $[Nn_3\Lambda]K^\pi$ of the dominant Nilsson component in the given HF state.

Nucleus	Spin ($\hbar$)	Q_2 (b)	γ (°)	Dominant component
^{185}Re$_{110}$	2.50	15.2	0.0	$[402]5/2^+$
^{187}Re$_{112}$	2.40	15.2	8.8	$[402]5/2^+$
^{189}Re$_{114}$	2.18	13.8	15.3	$[402]5/2^+$
^{191}Re$_{116}$	0.32	13.0	34.5	$[411]1/2^+$

The HF+SVI calculations predict that the γ deformations of the lowest-lying states increase from 0° in ^{185}Re to 35° in ^{191}Re (see Table 2). For the $[514]9/2^-$ levels, which are associated with the 18th negative-parity orbital, the values of γ are estimated to be 10° in ^{187}Re, 19° in ^{189}Re, and 31° in ^{191}Re, consistent with those derived from the signature splitting of the corresponding rotational bands in comparison with a particle-plus-triaxial-rotor model [43]. As such, all these arguments point to the occurrence of shape transition from axial symmetry to axial asymmetry as the neutron number increases towards $N = 116$ in the Re isotopic chain.

In a similar way, the low-lying levels of an $N = 117$ isotone ^{193}Os have been calculated to confirm the validity of the SVI interaction for neutron orbitals. The 31st negative-parity orbital (see the upper panel of Fig. 5) occupied by the last unpaired neutron is involved in the ground-state configuration for ^{193}Os. At the predicted deformation $Q_2 = 11.5$ b and $\gamma = 24°$, this neutron orbital is characterized with the asymptotic quantum numbers $[512]3/2^-$ of the largest component in the wave function, in agreement with the experimentally observed $3/2^-$ ground state of ^{193}Os [44]. The HF+SVI calculation also predicts that a $13/2^+$ state emerges at low excitation energy from the occupation of the 29th positive-parity orbital with $Q_2 = 11.8$ b and $\gamma = 35°$. Such a level has not been observed for ^{193}Os so far [44], but the analogous state has been identified recently as a long-lived ($T_{1/2} = 47 \pm 3$ s) isomer in ^{195}Os [26].

It is noteworthy that there are sizable gaps at $N = 116$ and $Z = 76$ around $\gamma = 30°$ in the SPE diagram shown in Fig. 5. The presence of such deformed energy gaps tends to enhance axial asymmetry, leading either to rigid triaxiality or to γ softness, or intermediate between them, in ^{192}Os and its vicinity.

Of particular interest is to see what configuration and shape degrees of freedom the odd-odd $N = 117$ nucleus ^{192}Re has in its

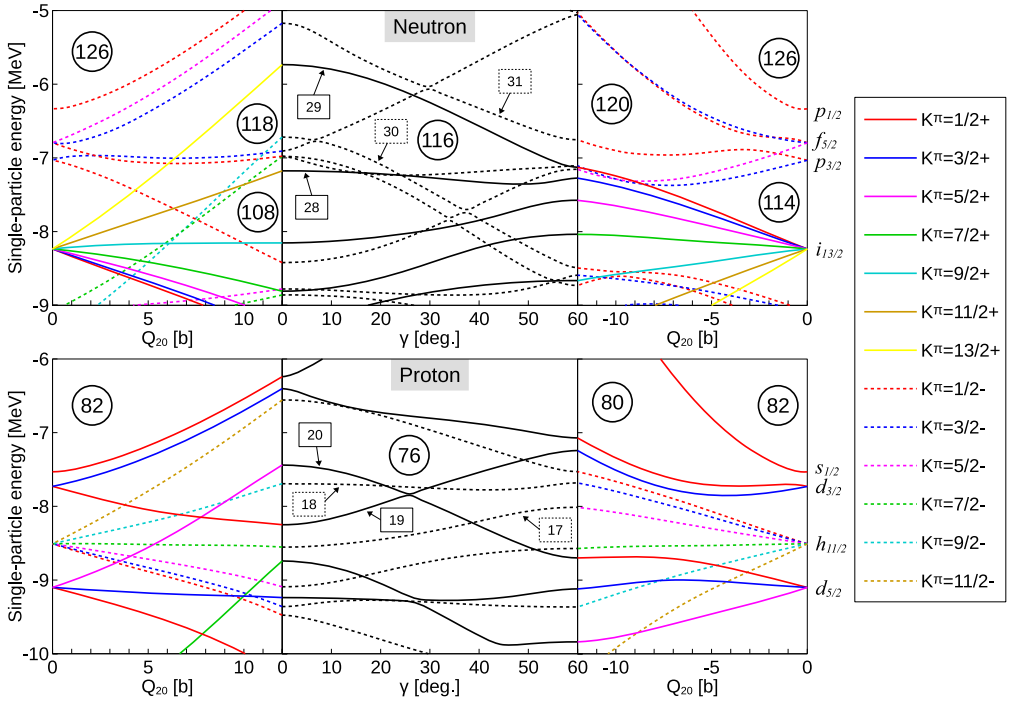

Fig. 5. Single-particle energies (SPEs) for neutrons (upper panel) and protons (lower panel) in ^{192}Os calculated with the Skyrme SVI interaction. In the left and right parts of the diagram, the SPEs are depicted as a function of the axial quadrupole moment Q_{20} from 0 to 12 b and from -12 to 0 b, respectively. In the middle part, the SPEs are depicted as a function of the degree of triaxial deformation γ for fixed $Q_{20} = 12$ b. The solid and dashed lines represent positive- and negative-parity states, respectively. For axial cases, states with different K^π quantum numbers are displayed in different colors, as indicated in the rightmost panel. For triaxial cases, several key orbitals relevant to the discussion are indicated by the numbers in squares, which are counted from the bottom of the potential well for the respective parities.

Table 3
Calculated spins, parities, excitation energies E_x, intrinsic quadrupole moments Q_2, and degrees of triaxial deformation γ for configurations denoted by the numbers of single-neutron (ν) and single-proton (π) states occupied in four parity-signature ($\pi = \pm 1, r = \pm i$) blocks, [$N(+1,+i)$, $N(+1,-i)$, $N(-1,+i)$, $N(-1,-i)$], for ^{192}Re. Two configurations in the same partition correspond to the ν-π spin-flip partners.

Configuration	Spin ($\hbar$)	Parity	E_x (keV)	Q_2 (b)	γ (°)
$\nu[28,28,30,31] \otimes \pi[20,20,17,18]$	3.67	+1	208	11.8	24.1
$\nu[28,28,30,31] \otimes \pi[20,20,18,17]$	4.99	+1	240	11.8	24.2
$\nu[28,29,30,30] \otimes \pi[19,20,18,18]$	6.61	+1	23	12.4	38.7
$\nu[28,29,30,30] \otimes \pi[20,19,18,18]$	5.98	+1	0	12.4	38.7
$\nu[28,28,30,31] \otimes \pi[19,20,18,18]$	0.64	-1	224	12.4	37.3
$\nu[28,28,30,31] \otimes \pi[20,19,18,18]$	0.09	-1	293	12.4	37.3
$\nu[28,29,30,30] \otimes \pi[20,20,17,18]$	10.4	-1	213	12.0	35.0
$\nu[28,29,30,30] \otimes \pi[20,20,18,17]$	2.42	-1	351	12.0	35.4

ground state, which has been experimentally assigned a spin and parity of (0^-) in the present work. The results of the HF+SVI calculations for low-energy excitations in ^{192}Re are summarized in Table 3, where the configurations are expressed as a set of the orbital numbers for both neutrons and protons in four parity-signature blocks. The configuration listed in the sixth row in Table 3 gives rise to nearly null spin with negative parity, and therefore, this state is the most probable candidate for the observed (0^-) ground state of ^{192}Re. (For the HF states calculated with the absence of the pairing correlations, uncertainties in energy of the order of several hundreds of keV are tolerable.) The predicted γ deformation for the 0^- state follows the increasing trend in the Re isotopes (see Table 2) beyond the maximum axial asymmetry at $\gamma = 30°$. This observation implies that the nuclear deformation is driven towards an oblate shape in the heavier Re isotopes, which have a significant impact on the formation of the 3rd-abundance peak around $A = 195$ in the rapid-neutron capture process [45], when approaching the $N = 126$ shell closure.

In Table 3, there are high-spin ($J \approx 7$, 10) states predicted to emerge at low excitation energy, which are likely to be long-lived due to the large difference in spin from the $J^\pi = (0^-)$ ground state. The previously identified isomers in ^{192}Re [18,19] might arise from these configurations, though their decay properties remain a challenge for future experiments.

To summarize, ^{192}Re is located close to the predicted critical point of a prolate-to-oblate shape transition via enhanced axial asymmetry in the neutron-rich $A \approx 190$ region. We have performed decay spectroscopy of this rare, refractory isotope using the newly developed KISS setup at RIKEN. Apparent β feedings to the known levels in ^{192}Os and the corresponding $\log ft$ values have been evaluated for the first time, whereby a spin and parity of 0^- are assigned tentatively for the ^{192}Re ground state. The low-energy level systematics for the neighboring odd-A nuclei can be explained as being ascribed to the variation of single-particle energies with triaxial deformation γ, indicative of the shape transition from prolate-axial symmetry to axial asymmetry approaching $N = 116$. The (0^-) ground state in ^{192}Re is predicted to have a

shape exceeding the maximum axial asymmetry at $\gamma = 30°$, suggesting that the nuclear deformation evolves to an oblate shape in heavier Re isotopes. A future experimental challenge is to measure nuclear moments of the Re isotopes to pin down the structural evolution discussed in this Letter.

Declaration of competing interest

The authors declare that they have no known competing financial interests or personal relationships that could have appeared to influence the work reported in this paper.

Acknowledgements

We thank the staff at RIKEN, RIBF for providing the excellent beams. This work was supported by JSPS KAKENHI Grant Nos. JP23244060, JP24740180, JP26247044, JP15H02096, JP17H01132, JP17H06090, and JP18H03711; the U.S. DOE, Office of Nuclear Physics under Award No. DE-AC02-06CH11357; the European Research Council (ERC) under the European Union's Horizon 2020 research and innovation programme (grant agreement No. 682841 "ASTRUm"); the UK Science and Technology Facilities Council under grant No. ST/L005743/1.

References

[1] A. Bohr, B. Mottelson, Nuclear Structure: Volume 2, Nuclear Deformations, Benjamin, 1975.
[2] S. Åberg, H. Flocard, W. Nazarewicz, Annu. Rev. Nucl. Part. Sci. 40 (1990) 439.
[3] J. Skalski, S. Mizutori, W. Nazarewicz, Nucl. Phys. A 617 (1997) 282.
[4] S. Ćwiok, P. Heenen, W. Nazarewicz, Nature 433 (2005) 705.
[5] P. Möller, R. Bengtsson, B.G. Carlsson, P. Olivius, T. Ichikawa, Phys. Rev. Lett. 97 (2006) 162502.
[6] L.M. Robledo, R. Rodríguez-Guzmán, P. Sarriguren, J. Phys. G, Nucl. Part. Phys. 36 (2009) 115104.
[7] G. Dracoulis, G. Lane, A. Byrne, H. Watanabe, R. Hughes, F. Kondev, M. Carpenter, R. Janssens, T. Lauritsen, C. Lister, D. Seweryniak, S. Zhu, P. Chowdhury, Y. Shi, F. Xu, Phys. Lett. B 720 (2013) 330.
[8] C.Y. Wu, D. Cline, T. Czosnyka, A. Backlin, C. Baktash, R.M. Diamond, G.D. Dracoulis, L. Hasselgren, H. Kluge, B. Kotlinski, J.R. Leigh, J.O. Newton, W.R. Phillips, S.H. Sie, J. Srebrny, F.S. Stephens, Nucl. Phys. A 607 (2) (1996) 178.
[9] K. Nomura, T. Otsuka, R. Rodríguez-Guzmán, L.M. Robledo, P. Sarriguren, P.H. Regan, P.D. Stevenson, Z. Podolyák, Phys. Rev. C 83 (2011) 054303.
[10] K. Nomura, N. Shimizu, D. Vretenar, T. Nikšić, T. Otsuka, Phys. Rev. Lett. 108 (2012) 132501.
[11] C.M. Baglin, Nucl. Data Sheets 113 (8) (2012) 1871.
[12] N. Al-Dahan, P.H. Regan, Z. Podolyák, P.M. Walker, N. Alkhomashi, G.D. Dracoulis, G. Farrelly, J. Benlliure, S.B. Pietri, R.F. Casten, P.D. Stevenson, W. Gelletly, S.J. Steer, A.B. Garnsworthy, E. Casarejos, J. Gerl, H.J. Wollersheim, J. Grebosz, M. Górska, I. Kojouharov, H. Schaffner, A. Algora, G. Benzoni, A. Blazhev, P. Boutachkov, A.M. Bruce, I.J. Cullen, A.M. Denis Bacelar, A.Y. Deo, M.E. Estevez, Y. Fujita, R. Hoischen, R. Kumar, S. Lalkovski, Z. Liu, P.J. Mason, C. Mihai, F. Molina, D. Mücher, B. Rubio, A. Tamii, S. Tashenov, J.J. Valiente-Dobón, P.J. Woods, Phys. Rev. C 85 (2012) 034301.
[13] http://www-phynu.cea.fr/science_en_ligne/carte_potentiels_microscopiques/noyaux/zz75/zz75n117all_eng.html.
[14] P.M. Walker, F.R. Xu, Phys. Rev. C 74 (2006) 067303.
[15] T. Nakamura, H. Sakurai, H. Watanabe, Prog. Part. Nucl. Phys. 97 (2017) 53.
[16] H. Watanabe, Eur. Phys. J. A 55 (2019) 19.
[17] T. Kurtukian-Nieto, J. Benlliure, K.-H. Schmidt, L. Audouin, F. Becker, B. Blank, E. Casarejos, F. Farget, M. Fernández-Ordóñez, J. Giovinazzo, D. Henzlova, B. Jurado, J. Pereira, O. Yordanov, Phys. Rev. C 89 (2014) 024616.
[18] M. Caamano, P.M. Walker, P.H. Regan, M. Pfützner, Zs. Podolyák, J. Gerl, M. Hellström, P. Mayet, M.N. Mineva, A. Aprahamian, J. Benlliure, A.M. Bruce, P.A. Butler, D. Cortina Gil, D.M. Cullen, J. Döring, T. Enqvist, C. Fox, J. Garcés Narro, H. Geissel, W. Gelletly, J. Giovinazzo, M. Górska, H. Grawe, R. Grzywacz, A. Kleinböhl, W. Korten, M. Lewitowicz, R. Lucas, H. Mach, C.D. OĹeary, F. De Oliveira, C.J. Pearson, F. Rejmund, M. Rejmund, M. Sawicka, H. Schaffner, C. Schlegel, K. Schmidt, K.-H. Schmidt, P.D. Stevenson, Ch. Theisen, F. Vivès, D.D. Warner, C. Wheldon, H.J. Wollersheim, S. Wooding, F. Xu, O. Yordanov, Eur. Phys. J. A 23 (2005) 201.
[19] M.W. Reed, P.M. Walker, I.J. Cullen, Y.A. Litvinov, D. Shubina, G.D. Dracoulis, K. Blaum, F. Bosch, C. Brandau, J.J. Carroll, D.M. Cullen, A.Y. Deo, B. Detwiler, C. Dimopoulou, G.X. Dong, F. Farinon, H. Geissel, E. Haettner, M. Heil, R.S. Kempley, R. Knöbel, C. Kozhuharov, J. Kurcewicz, N. Kuzminchuk, S. Litvinov, Z. Liu, R. Mao, C. Nociforo, F. Nolden, W.R. Plaß, Z. Podolyak, A. Prochazka, C. Scheidenberger, M. Steck, T. Stöhlker, B. Sun, T.P.D. Swan, G. Trees, H. Weick, N. Winckler, M. Winkler, P.J. Woods, F.R. Xu, T. Yamaguchi, Phys. Rev. C 86 (2012) 054321.
[20] V. Zagrebaev, W. Greiner, Phys. Rev. Lett. 101 (2008) 122701.
[21] Y.X. Watanabe, Y.H. Kim, S.C. Jeong, Y. Hirayama, N. Imai, H. Ishiyama, H.S. Jung, H. Miyatake, S. Choi, J.S. Song, E. Clement, G. de France, A. Navin, M. Rejmund, C. Schmitt, G. Pollarolo, L. Corradi, E. Fioretto, D. Montanari, M. Niikura, D. Suzuki, H. Nishibata, J. Takatsu, Phys. Rev. Lett. 115 (2015) 172503.
[22] Y. Hirayama, Y. Watanabe, N. Imai, H. Ishiyama, S. Jeong, H. Miyatake, M. Oyaizu, S. Kimura, M. Mukai, Y. Kim, T. Sonoda, M. Wada, M. Huyse, Y. Kudryavtsev, P.V. Duppen, Nucl. Instrum. Methods Phys. Res. B 353 (2015) 4.
[23] Y. Hirayama, Y. Watanabe, N. Imai, H. Ishiyama, S. Jeong, H. Jung, H. Miyatake, M. Oyaizu, S. Kimura, M. Mukai, Y. Kim, T. Sonoda, M. Wada, M. Huyse, Y. Kudryavtsev, P.V. Duppen, Nucl. Instrum. Methods Phys. Res. B 376 (2016) 52.
[24] Y. Hirayama, Y. Watanabe, M. Mukai, M. Oyaizu, M. Ahmed, H. Ishiyama, S. Jeong, Y. Kakiguchi, S. Kimura, J. Moon, J. Park, P. Schury, M. Wada, H. Miyatake, Nucl. Instrum. Methods Phys. Res. B 412 (2017) 11.
[25] Y. Hirayama, Y. Watanabe, M. Mukai, P. Schury, M. Ahmed, H. Ishiyama, S. Jeong, Y. Kakiguchi, S. Kimura, J. Moon, M. Oyaizu, J. Park, M. Wada, H. Miyatake, Nucl. Instrum. Methods Phys. Res. B 463 (2020) 425.
[26] Y.X. Watanabe, M. Ahmed, Y. Hirayama, M. Mukai, J.H. Park, P. Schury, Y. Kakiguchi, S. Kimura, A. Ozawa, M. Oyaizu, M. Wada, H. Miyatake, Phys. Rev. C 101 (2020) 041305.
[27] M. Mukai, Y. Hirayama, Y. Watanabe, P. Schury, H. Jung, M. Ahmed, H. Haba, H. Ishiyama, S. Jeong, Y. Kakiguchi, S. Kimura, J. Moon, M. Oyaizu, A. Ozawa, J. Park, H. Ueno, M. Wada, H. Miyatake, Nucl. Instrum. Methods Phys. Res., Sect. A 884 (2018) 1.
[28] A. Akber, M.W. Reed, P.M. Walker, Y.A. Litvinov, G.J. Lane, T. Kibédi, K. Blaum, F. Bosch, C. Brandau, J.J. Carroll, D.M. Cullen, I.J. Cullen, A.Y. Deo, B. Detwiler, C. Dimopoulou, G.D. Dracoulis, F. Farinon, H. Geissel, E. Haettner, M. Heil, R.S. Kempley, R. Knöbel, C. Kozhuharov, J. Kurcewicz, N. Kuzminchuk, S. Litvinov, Z. Liu, R. Mao, C. Nociforo, F. Nolden, W.R. Plaß, Z. Podolyák, A. Prochazka, C. Scheidenberger, D. Shubina, M. Steck, T. Stöhlker, B. Sun, T.P.D. Swan, G. Trees, H. Weick, N. Winckler, M. Winkler, P.J. Woods, T. Yamaguchi, Phys. Rev. C 91 (2015) 031301.
[29] M. Wang, G. Audi, F.G. Kondev, W. Huang, S. Naimi, X. Xu, Chin. Phys. C 41 (2017) 030003.
[30] T. Kibédi, T. Burrows, M. Trzhaskovskaya, P. Davidson, C. Nestor, Nucl. Instrum. Methods Phys. Res., Sect. A 589 (2008) 202.
[31] W. Kane, R. Casten, D. Warner, K. Schreckenbach, H. Faust, S. Blakeway, Phys. Lett. B 117 (1982) 15.
[32] B. Singh, J. Rodriguez, S. Wong, J. Tuli, Nucl. Data Sheets 84 (1998) 487.
[33] J. Jansen, H. Pauw, C. Toeset, Nucl. Phys. A 115 (1968) 321.
[34] C. Hirning, D. Burke, E. Flynn, J. Sunier, P. Schmelzbach, R. Haglund, Nucl. Phys. A 287 (1977) 24.
[35] R. Rodríguez-Guzmán, P. Sarriguren, L.M. Robledo, J.E. García-Ramos, Phys. Rev. C 81 (2010) 024310.
[36] P. Sarriguren, R. Rodríguez-Guzmán, L.M. Robledo, Phys. Rev. C 77 (2008) 064322.
[37] https://www.fuw.edu.pl/~dobaczew/hfodd/hfodd.html.
[38] N. Schunck, J. Dobaczewski, W. Satula, P. Baczyk, J. Dudek, Y. Gao, M. Konieczka, K. Sato, Y. Shi, X. Wang, T. Werner, Comput. Phys. Commun. 216 (2017) 145.
[39] M. Beiner, H. Flocard, N. Van Giai, P. Quentin, Nucl. Phys. A 238 (1) (1975) 29.
[40] J. Bartel, P. Quentin, M. Brack, C. Guet, H.-B. Hakansson, Towards a better parametrisation of skyrme-like effective forces: a critical study of the skm force, Nucl. Phys. A 386 (1982) 79.
[41] E. Chabanat, P. Bonche, P. Haensel, J. Meyer, R. Schaeffer, Nucl. Phys. A 627 (1997) 710.
[42] J. Dobaczewski, H. Flocard, J. Treiner, Nucl. Phys. A 422 (1984) 103.
[43] M. Reed, G. Lane, G. Dracoulis, F. Kondev, M. Carpenter, P. Chowdhury, S. Hota, R. Hughes, R. Janssens, T. Lauritsen, C. Lister, N. Palalani, D. Seweryniak, H. Watanabe, S. Zhu, W. Jiang, F. Xu, Phys. Lett. B 752 (2016) 311.
[44] M. Shamsuzzoha Basunia, Nucl. Data Sheets 143 (2017) 1.
[45] E.M. Burbidge, G.R. Burbidge, W.A. Fowler, F. Hoyle, Rev. Mod. Phys. 29 (1957) 547.